Indian Journal of Geo Marine Sciences
Vol. 51 (05), May 2022, pp. 459-467
DOI: 10.56042/ijms.v51i05.65571

Adsorption of chromium from aqueous solution using Chitosan-g-Graphene/Hydroxyapatite composite

V Geetha[a], S Latha[b], T Gomathi[c], S Pavithra[c] & P N Sudha*[,c]

[a]Department of Chemistry, Bharathiar university, Coimbatore, Tamil Nadu – 641 046, India

[b]School of Advanced Sciences, VIT University, Vellore, Tamilnadu – 632 014, India

[c]PG and Research Department of Chemistry, DKM College for Women, Vellore, Tamil Nadu – 632 001, India

*[E-mail: drparsu8@gmail.com]

Received 04 February 2022; revised 07 May 2022

The preparation and characterisation of a polymeric composite incorporating graphene, hydroxyapatite, and chitosan as an adsorbent to remove chromium (VI) from wastewater. The FTIR and XRD studies supported the composite's production. Analysis of surface morphology and heat stability involved TGA and SEM studies. A batch adsorption was run to determine the efficacy of the adsorbent by varying contact time, adsorbent dose, and pH. The kinetics of the adsorption process were examined using pseudo-first and second order kinetic models after the equilibrium data had been fitted with the Langmuir and Freundlich isotherms. The findings showed that pseudo second order kinetics was utilised for the adsorption of Cr(VI) onto chitosan-grafted graphene/hydroxyapatite (CS-g-Gr/HA) composite.

[**Keywords**: Adsorption, Chitosan, Chromium, Composite, Graphene, Hydroxyapatite]

Introduction

All living things, including people, animals, and the environment, depend on water. The earth's surface is covered in water to the tune of seventy percent; 96.5 percent of which is salt water. Due to industrial expansion, urbanization and agricultural practices surface water is getting polluted with toxic metals such as Cr, Pb, Hg and Cd. Intake of heavy metals above the accepted limits will cause serious health problems to all living beings. Among the various toxic heavy metals, chromium toxicity causes various incurable diseases. Therefore, the present research focuses on Chromium heavy metal, which can cause gastro intestinal disorders, convulsions, genetic disorders and cancer in human beings[1]. This heavy metal chromium gets released to water bodies through leather tanning, mining, electroplating, paints, pigments, power generation plants and textile industries[2-4]. The two oxidation states of chromium are Cr (III), (VI), with the latter being more hazardous than the former. Low levels of chromium can irritate the skin and lead to ulcers. Long-term exposure can harm the kidneys, the liver, the nervous system, and the circulatory system. Again, it's critical to eliminate such Cr residues from effluent[5,6].

Several processes, including chemical precipitation, oxidation/reduction, filtering, ion exchange, membrane separation, and adsorption, can remove heavy metals from water[7]. Adsorption was preferred to the other technologies because of its low cost and excellent efficiency. Adsorption is a relatively simple process wherein an adsorbate gets adsorbed on to the adsorbent through chemical or physical bonding[8,9]. Many adsorbents such as sawdust[10], activated carbon[11], surfactant modified Zeolite[12], carbon/ AlOOH composite[13], cellulose extracted from sisal fiber[14], clay materials[15,16], and chitosan[17-20] were generally used to adsorb Cr. Whereas, the chitin and chitosan have been extensively used to remove chromium in the effective manner from the wastewater and also it has been used in various fields like biotechnology, biomedicine and food ingredients because it is biocompatible[21-23]. Chitosan is an alpha-D-glucosamine-linked form of chitin that has been partially or totally deacetylated. Because it contains hydroxyl and amino groups, which the amine groups use as chelate site for transition metal ions, it can function as a powerful biosorbent. Because of its weak mechanical qualities and acidic solubility, chitosan a good biosorbent with many desirable qualities must be modified. Chitosan can also be chemically modified, such as via crosslinking and grafting, to increase its chemical stability and adsorption capability[24-26].

Apart from Chitosan (CS), Hydroxyapatite (HA) and Graphene (Gr) are also studied as adsorbents for

heavy metal ions[27-30]. HA has similar composition as that of bone and teeth, and is widely studied when it comes to tissue engineering, food processing, adsorption and so on. HA, the inorganic material when combined with organic matrix can serve as a composite of good mechanical strength. Also the OH group and Calcium ions present in HA will contribute for more adsorption. A number of researchers have become interested in graphene because of its superior mechanical strength and bigger surface area. One of the key elements in an adsorbent's ability to effectively absorb is surface area. Greater the surface area more will be the adsorbing sites and greater is the adsorption. The proposed study's goal is to create an innovative and effective Chitosan-grafted Graphene/Hydroxyapatite (CS-g-Gr/HA) composite that can be used as a Cr adsorbent. Chitosan is combined with HA and Graphene and crosslinked with glutaraldehyde to achieve high chemical stability and adsorption capability. Through batch adsorption tests, the prepared material was characterised and its adsorption potential was measured.

Materials and Methods

Chitosan, which is 92 % deacetylated, was a procured from India Sea Foods in Cochin. The supplier of graphene was Nano Beach in New Delhi. Acetic acid and glutaraldehyde were bought from SD Fine Chemicals, and HA was purchased from Leochem in Bangalore.

Preparation of Chitosan grafted Graphene/Hydroxyapatite (CS-g-Gr/HA) composite

1 g of CS was weighed and dissolved in acetic acid at a 2 percent concentration. 0.2 g of Gr and 0.1 g of HA were weighed simultaneously and separately before being dissolved in a small volume of deionized water. Separately, the dispersed HA and Gr were gradually added to the CS suspension one at a time. Next, 7 ml of glutaraldehyde was added, and the mixture in magntic stirrer. The materials were moved to the petriplates and given time to air-dry[31].

Characterization

An Alpha Bruker used for (FT-IR) spectra in the 400–4000 cm^{-1} wavelength range. An X-ray scattering D8 ADVANCE. To examine the weight losses at various phases, the produced extracts were analysed for a TGA analysis utilising an SDT Q600 V8.0. SEM has been used to examine the surface morphology of prepared composites.

Batch adsorption experiment

The adsorbent was stirred with potassium dichromate solution (200 mg/L). By adjusting variables including pH by using 0.1 N NaOH, HCL (between 4 and 8), adsorbent dose (between 1-6 g), and time, the extent of chromium adsorption was examined (60–360 min). After adsorption, whatmann filter paper was used to filter the solution, and it was then dried. The filtered concentration of chromium was determined using an AAS.

Results and Discussion

Characterization of the CS-g-Gr/HA composite

The FTIR spectra of pure CS and CS-g-Gr/HA composite are contrasted in Figure 1. The fingerprint of each polymer used to create the composite is visible in the spectrum. The peak at 1647 cm^{-1} indicates the presence of imine bond (N=C), which was formed due to crosslinking between CS and glutaraldehyde. The existence of Gr was confirmed by the high intensity peak at 1520 cm^{-1}, which was linked to an ethylenic bond (C=C) and showed enhanced intensity[32-34]. The disappearance of the CS peaks at 1384, 1151, and 1000 cm^{-1} indicates that CS interacted with HA (phosphate groups) and glutaraldehyde. The characteristic phosphate bending vibration of HA shows at 609 cm^{-1} and 504 cm^{-1}[refs. 35,36] confirming the miscibility of the mixed polymeric materials due to the formation of strong interaction. The OH and N-H stretching vibrations of CS was shifted from 3454 – 3517 cm^{-1}. This decrease in intensity and shift in the absoption band indicates that the OH group of both CS and HA were involved in weaker hydrogen bonding.

In the XRD of CS-g-Gr/HA composite (Fig. 2), the broadened peak indicates the amorphous nature. The crystalline nature of CS was decreased while grafting, blending and crosslinking with glutaraldehyde, Gr and HA. The composite showed peaks at 26° and 41° which corresponds to (002) (100) reflections of Gr. Pure CS exhibits a peak at 20° was shifted to 26° in the CS-g-Gr/HA composite and overlapped with grapheme (26°) and HAP (26°) peak. Also a broad peak around 30° was obtained from (211), (300), (202) diffractions of HA[37] confirms the confirms HA in the prepared composite. Additionally, the increased porousness of the composite as shown by the SEM pictures of the CS-g-Gr/HA composite confirms the XRD reflections. On comparing with the SEM image of pure chitosan, the prepared composite has rough

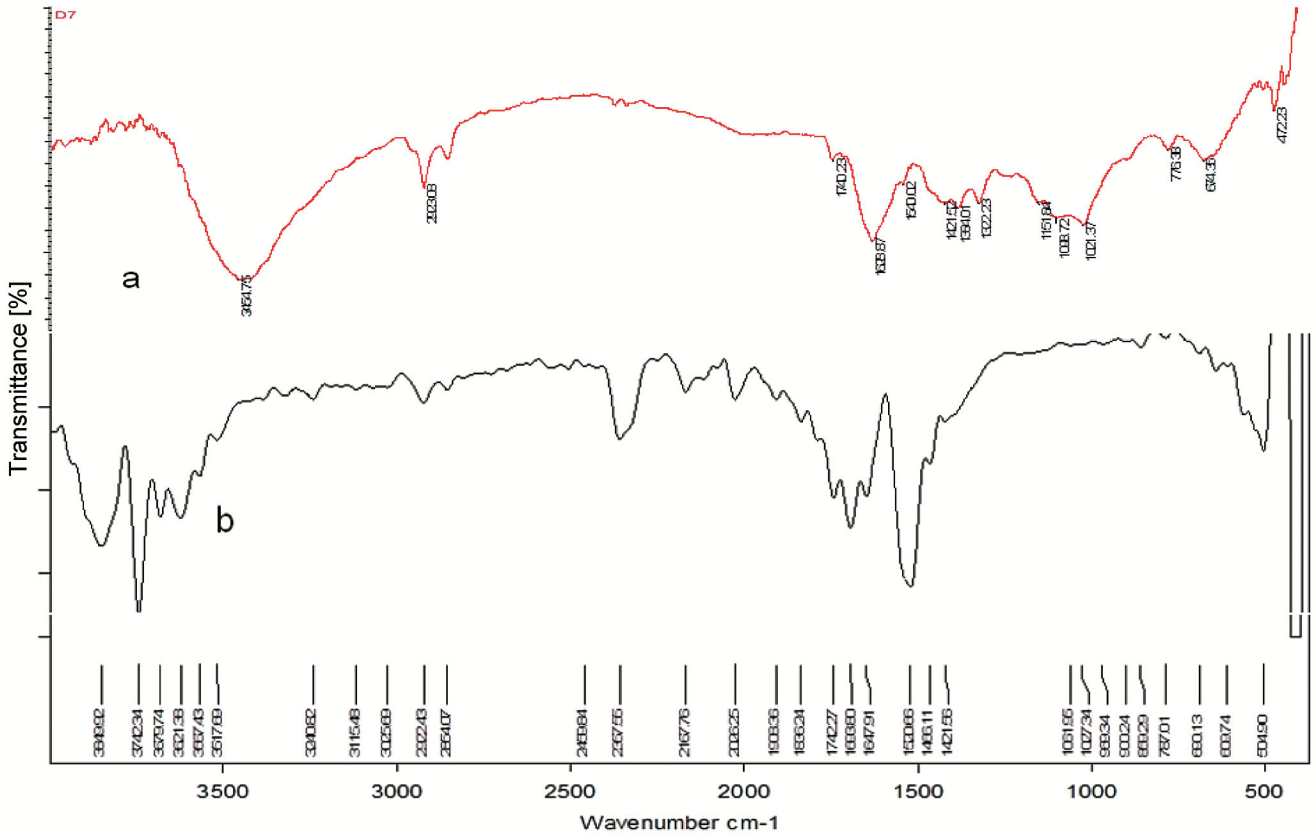

Fig. 1 — FTIR spectrum of (a) pure chitosan, and (b) CS-g-Gr/HA composite

surface morphology (Fig. 3a), layered structure with increased tunneling of porosity which is the essential property of the adsorbent.

TGA examination of the CS-g-Gr/HA composite's thermal stability was carried out, and the results were compared to those of pure chitosan. Figure 4 depicts the prepared CS-g-Gr/HA composite losing weight in four phases. Disruption of the absorbed water molecules caused the first stage, which was visible between 0 and 160 °C. At this temperature, very little weight loss (11.65 %) occurs, which is consistent with the composite's FTIR spectrum and confirms less hydrogen bonding. Between 160 °C and 315 °C, there was a significant weight loss of 23.10 percent, which is consistent with the breakdown of the cross-linked polymer structure. Between 380 °C and 550 °C, a third stage of weight loss of 22.84 percent was seen. A derivative peak with a temperature of 434.33 °C indicates that this is in accordance with the destruction of the glucosamine linkages of CS and the combustion of the carbon contained in Gr[38-40]. The DTG curve in the temperature range of 600 °C and 740 °C revealed the decomposition of HA at 681 °C. The three chemicals are all present, and the TGA study validates their breakdown temperatures.

The composite was also used as a chromium adsorbent to remove the heavy metal in various paratmeters.

Effect of pH

Figure 3(b) illustrates how pH affects the chromium adsorption by the CS-g-Gr/HA composite. As the pH of the solution from 4 to 6, the chromium adsorption was found to increase. The solution with low pH was created by adding hydrochloric acid, which lowered the pH to an acidic state (below 4) containing chromium ions as well as H^+ ions. The majority of the adsorbent site was occupied by these H^+ ions, and the amine groups of the adsorbent were also heavily protonated, which causes the electostatic repulsion of metal cations and adsorbent. The amount of H^+ ions declines from pH 4 to pH 6 while the amount of chromium ions increases. Because there are more adsorption sites available at pH 6, the amount of chromium that may be adsorbed is at its highest at pH 6. Reduced adsorption was seen because

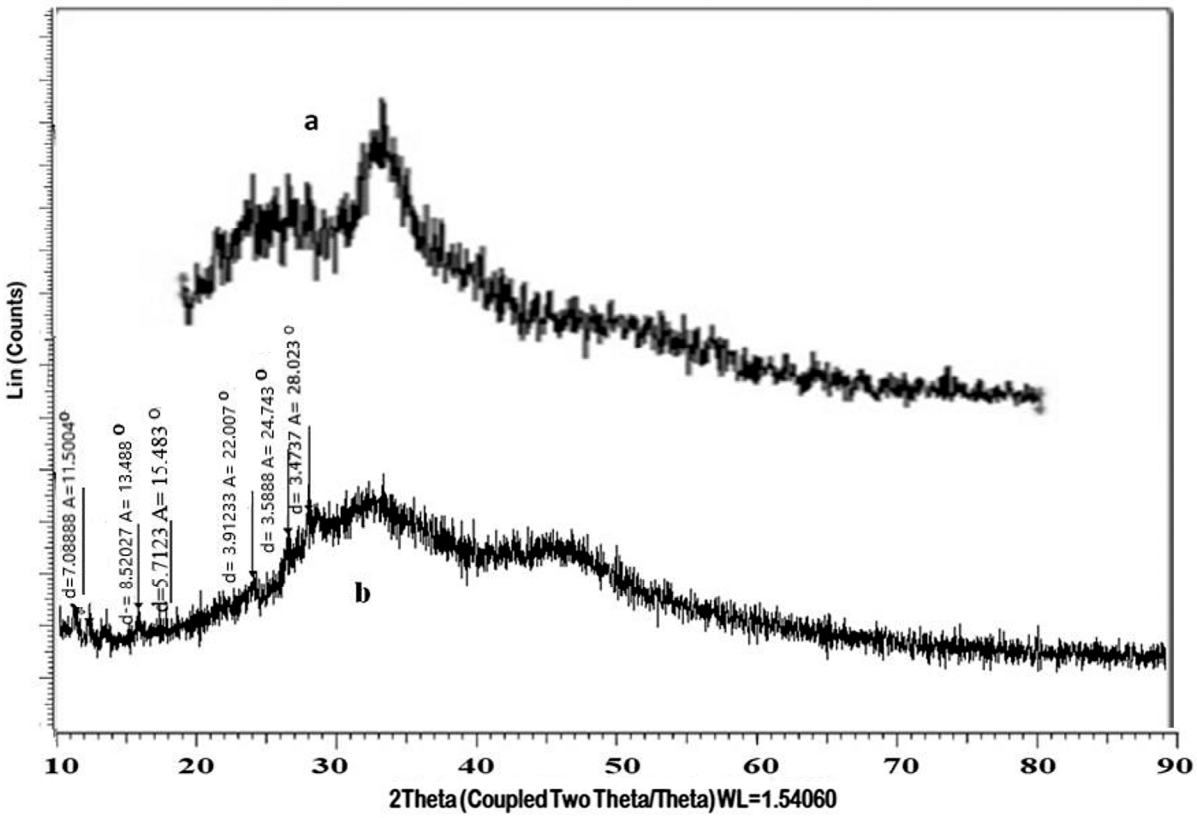

Fig. 2 — XRD pattern of (a) pure chitosan, and (b) CS-g-Gr/HA composite

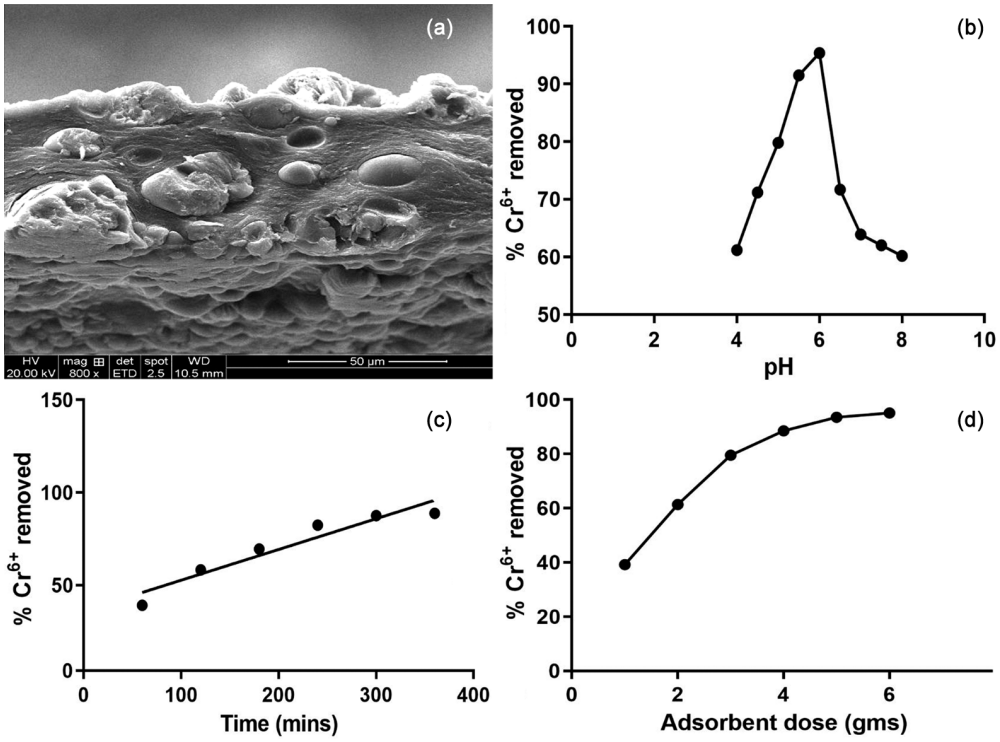

Fig. 3 — (a) SEM image of CS-g-Gr/HA, (b) Effect of pH, (c) Effect of contact time, and (d) Effect of adsorbent dose

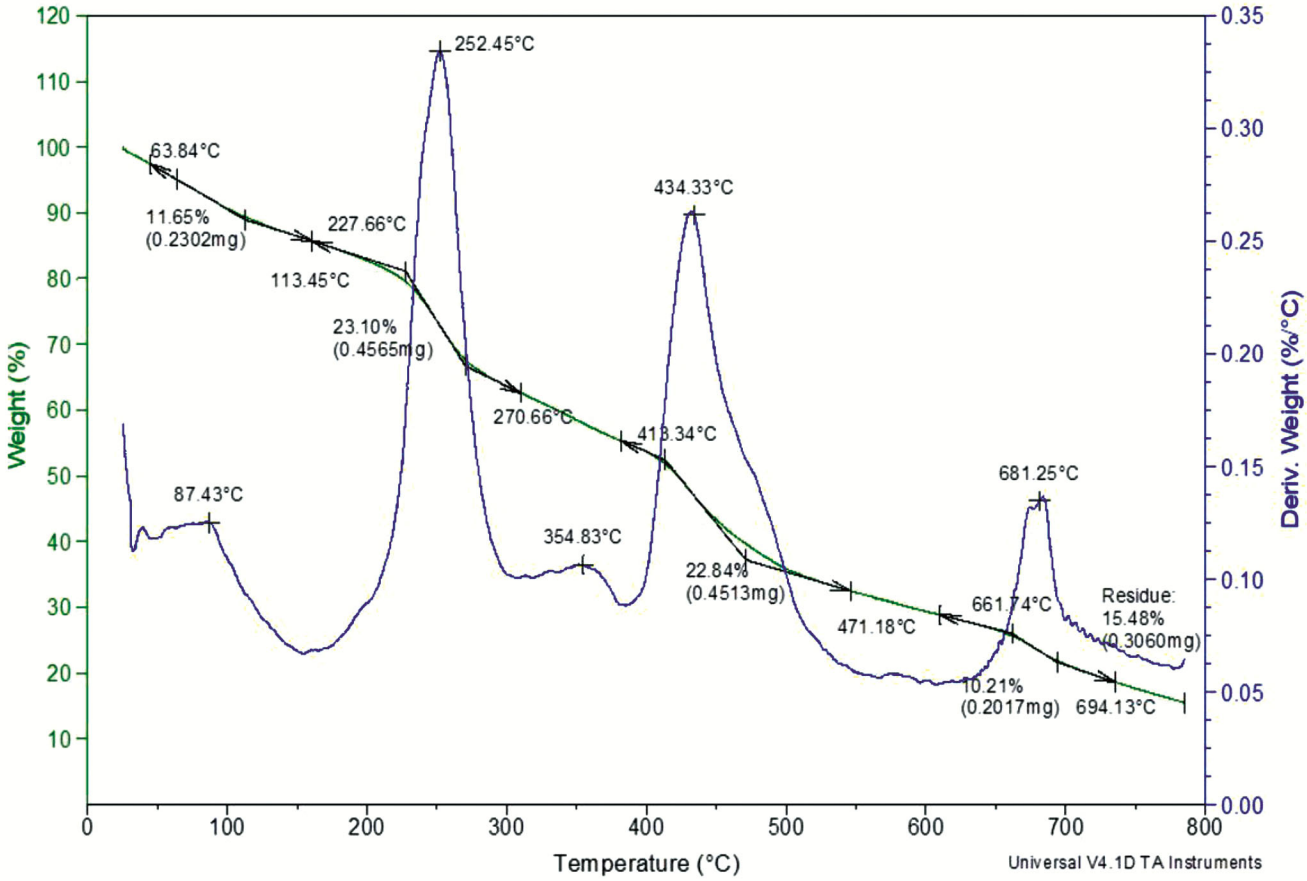

Fig. 4 — TGA thermogram of CS-g-Gr/HA

hydroxide complexes precipitate as the pH is raised further. The elimination of chromium was determined to be 95 % at the ideal pH level of 6.40.

Effect of contact time

Figure 3(c) demonstrates a quick rise in chromium adsorption as the duration rose from 60 min to 240 min, but no appreciable increase in adsorption as the time went further to 360 min. The reason for the significant expansion in adsorption is the increase in the number of vaccant adsorbent sites available for adsorption. As the adsorption proceeds, a finite number of adsorbing sites for the adsorbate remain in the adsorbent, leading to adsorption saturation.

Influence of adsorbent dose

To assess the adsorption of Cr(VI) from aqueous solution onto the composite, the number of adsorbents (1 to 6 g) was adjusted while maintaining the other variables (pH, contact duration) unchanged. It is clear from Figure 3(d) that as adsorbent dosage increases, so does Cr(VI) adsorption. An increase in active sites on the adsorbent causes a rise in adsorption. There was a supply of 4 g of the adsorbent after only a brief period of adsorption.

Adsorption isotherms

Langmuir isotherm model

The most commonly used isotherm was found to be Langmuir's adsorption isotherm. It is based on few assumptions that adsorption occurs at homogeneous surface and each of the adsorbent sites is capable of adsorbing one molecule of adsorbate resulting in one molecule thick of the adsorbed layer[41,42].

The linear form of the Langmuir isotherm follows:

$$C_{eq}/C_{ads} = bC_{eq}/K_L + 1/K_L \quad \ldots (1)$$

$$C_{max} = K_L/b \quad \ldots (2)$$

Figure 5 and the straight line it produces supports the isotherm's applicability. Equation allows for the determination of the constants b and K_L, which are features of the Langmuir equation (2). Figure depicts the Cr(VI) ion sorption by the composite of CS-g-Gr/HA using the Langmuir adsorption isotherm. Table 1 showed the Langmuir parameters values.

Table 1 — Langmuir and Freundlich isotherm parameters of CS-g-Gr/HA composite

	Langmuir constants				Freundlich constants		
Metal ion	K_L (dm^3/g)	b (dm^3/mg)	C_{max} (mg/g)	R^2	K_F (dm^3/g)	n (dm^3/mg)	R^2
Cr(VI)	1.2095	0.00957	126.4	0.7642	2.6382	1.5330	0.9829

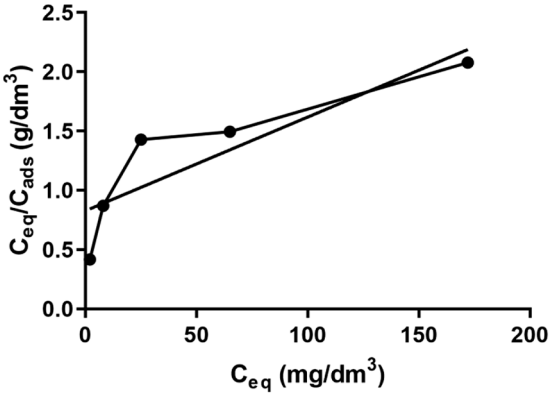

Fig. 5 — Langmuir isotherm model

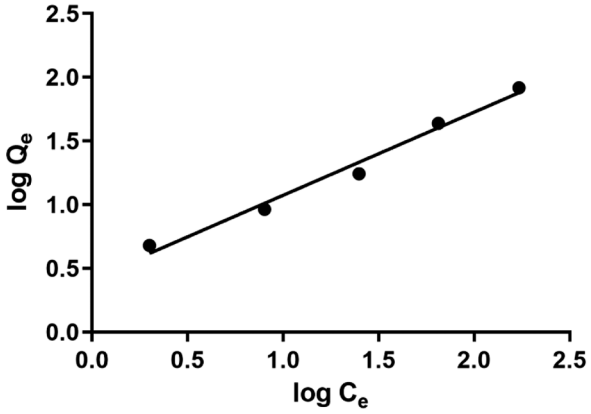

Fig. 6 — Freundlich isotherm model

Freundlich isotherm model

The linear form of Freundlich equation is expressed as:

$$\log q_e = \log K_F + 1/n \log C_e \quad \ldots (3)$$

Where, q_e = Amount adsorbed per g of adsorbent at equilibrium (mg g/1), C_e = Equilibrium concentration of adsorbate in solution following adsorption (mg dm^3), and K_f = Empirical Freundlich constant or capacity factor (mg g/1),

The 1/n ratios between 0 and 1 support the favourable adsorption conditions. Figure 6's linear plots demonstrate the Freundlich models' suitability. The Freundlich isotherm's n value was equal to 1.5330, which falls within the range of 1 to 10. This value denotes robust adsorption and suggests that metal ions physically adhered to the adsorbent[43].

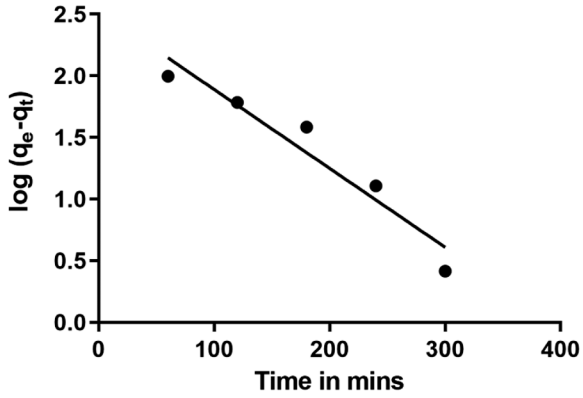

Fig. 7 — Pseudo first order kinetic model

The results of the current study's R^2 (0.7642) value showed that the graph was not linear and that the Langmuir equation was not applied successfully to support monolayer biosorption. When compared to the Langmuir model, the Freundlish isotherm has a greater correlation coefficient value (0.9829), indicating that the adsorption occurred more successfully on the multilayer surface.

Adsorption kinetics

Pseudo first order equation

Linear form of the pseudo-first-order follows[44]:

$$\log (q_e - q_t) = \log q_e - k_1 t / 2.303 \quad \ldots (4)$$

Where, the pseudo-first-order adsorption rate constant is k_1 (min^{-1}), and the amounts of metal adsorbed (mg/g) at equilibrium and time t, respectively. Rate constant graph shown in (Fig. 7).

Pseudo second order equation

The following is a representation of the pseudo-second-order rate equation.

$$\frac{t}{q_t} = \frac{1}{k_2 q_e^2} + \frac{t}{q_e} \quad \ldots (5)$$

Where, k_2 (g mg^{-1} min^{-1}) is the pseudo second order adsorption rate constant. A graph for the pseudo-second-order model is shown in Figure 8. Table 1 presents the results for kinetic models. The table demonstrates that the pseudo second order model's correlation coefficient value is higher than the pseudo first order model's.

Table 2 — Kinetic parameters of CS-g-Gr/HA composite

Metal ion	Pseudo-first-order kinetic model			Experimental value q_e (mg/g)	Pseudo-second-order kinetic model			Intraparticle diffusion	
	q_e (mg/g)	k_1 (min^{-1})	R^2		q_e (mg/g)	k_2 (g mg^{-1} min^{-1})	R^2	K_i (mg/g $h^{0.5}$)	R^2
Cr (VI)	395.18	0.006402	0.9269	192	130.04	0.003366	0.9943	10.27	0.9916

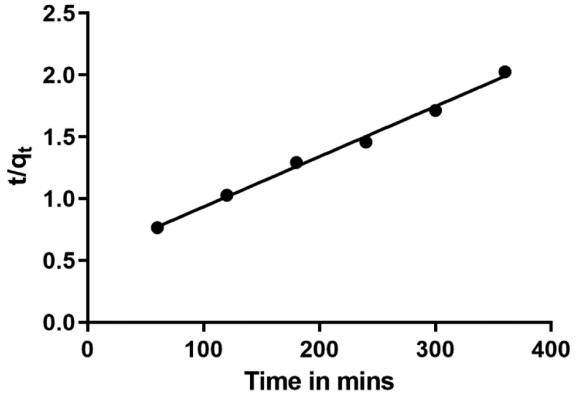

Fig. 8 — Pseudo second order kinetic model

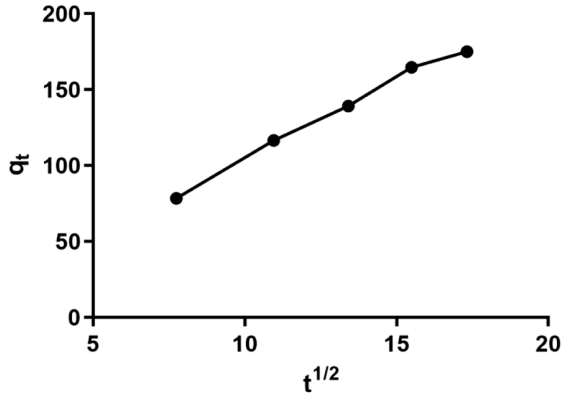

Fig. 9 — Intra particle diffusion model

Intra particle diffusion

The intra particle kinetic Weber-Morris model provides pertinent data regarding Cr (VI) ion diffusion in the finished composite. Equation $qt = K_{it}^{1/2}+C$ provides the mathematical expression for the intra particle kinetic model.

A straight line was produced when plotting q_t against $t_{1/2}$ and is depicted in Figure 9. The surface sorption makes a bigger contribution to the rate-determining step when C is larger. Because the linear portions of the curve did not cross through the origin, the cr adsorption on the composite was produced by both surface adsorption and intra-particle diffusion[45].

Table 2 according to the findings, the pseudo-first, second order R^2 = 09269, 0.9943 and intra particle diffusion model (R^2 = 0.9916), respectively.

Conclusion

The unique CS-g-Gr/HA composite that was created for this task was needed to remove the Cr (V) ion. From ideal pH, contact time, and adsorbent dose for efficient Cr(VI) adsorption are pH 6, 240 min, and 4 g, respectively. The outcomes showed that Cr(VI) adsorption increased quickly in the beginning and decreased as it approached equilibrium. The multilayer adsorption of Cr by the composite, which is indicated by the experimental results' good agreement with the Freundlich adsorption isotherm's R^2 = 0.9829 value over Langmuir's adsorption isotherm. Cr was adsorbed onto the CS-g-Gr/HA composite according to a pseudo-second order.

Acknowledgements

The authors would like to thank the management of DKM College for Women, Vellore for extending the facility to carry out this research.

Conflict of Interest

The authors declare that there is no conflict of interest.

Ethical Statement

This work was not published in any mean and no endangered species are being used in this study.

Author Contributions

VG: Experimental data analysis and manuscript writing; SL: Data analysis and data interpretation; TG: Manuscript formatting and Result interpretation; SP: Plagiarism and reference formatted; and PNS: Conceptualization and editing the manuscript.

References

1 *Guidelines for drinking-water quality*, 2nd edn, Vol 2, Health criteria and other supporting information, (World Health Organization, Geneva), 1996.

2 Leyva-Ramos R, Zacobo-Azuara A, Diaz-Flores P E, Guerrero-Coronado R M, Mendoza-Barron J, *et al*., Adsorption of cadmium (*II*) from aqueous solution onto activated carbon, *Colloids Surf A Physicochem Eng Asp*, 330 (2008) 35–41.

3 Manjeet B, Diwan S & Garg V K, A comparative study for the removal of hexavalent chromium from aqueous solution by agriculture wastes' carbons, *J Hazard Mater*, 171 (2009) 83–92.

4 Schneider R M, Cavalin C F, Barros M A S D & Tavares C R G, Adsorption of chromium ions in activated carbon, *Chem Eng J*, 132 (2007) 355–362.

5 Ronak B, Sreedhar B & Padmaja P, Adsorption of chromium from aqueous solutions using crosslinked chitosan–diethylenetriaminepentaacetic acid, *Int J Biol Macromolec*, 74 (2015) 458-466.

6 Mubarak N M, Sahu J N, Abdullah E C & Jayakumar N S, Removal of Heavy Metals from Wastewater Using Carbon Nanotubes, *Sep Purif Rev*, 43 (2014) 311–338.

7 Rengaraj S, Yeon K H & Moon S H, Removal of chromium from water and wastewater by ion exchange resins, *J Hazard Mater*, 87 (2001) 273–287.

8 Xiaoshu L, Jiang X, Guangming J, Jie T & Xinhua X, Highly active nanoscale zero-valent iron (nZVI)–Fe_3O_4 nanocomposites for the removal of chromium(VI) from aqueous solutions, *J Colloid Interface Sci*, 369 (2012) 460-469.

9 Hajeeth T, Vijayalakshmi K, Gomathi T & Sudha P N, Removal of Cu(II) and Ni(II) using cellulose extracted from sisal fiber and cellulose-g-acrylic acid copolymer, *Int J Biol Macromolec*, 62 (2013) 59-65.

10 Suresh G & Babu B V, Experimental Investigations and Theoretical Modeling Aspects in Column Studies for Removal of Cr(VI) from Aqueous Solutions Using Activated Tamarind Seeds, *Chem Eng J*, 150 (2009) 352-365.

11 Leyva-Ramos R & Juarez-Martinez A, Guerrero-coronado, RM, Adsorption of Chromium(VI) from aqueous solutions on activated carbon, *Water Sci Tech*, 30 (1994) 191-197.

12 Leyva-Ramos R, Jacobo-Azuara A, Diaz-Flores P E, Guerrero-Coronado R M, Mendoza-Barron J, *et al.*, Adsorption of Chromium(VI) from an aqueous solution on a surfactant – modified zeolite, *Colloids Surf A Physicochem Eng Asp*, 330 (2008) 35-41.

13 Rajeev K, Muhammad E & Barakat M A, Synthesis and Characterization of carbon/AlOOH composite for adsorption of chromium(VI) from synthetic waste water, *J Ind Eng Chem*, 20 (2014) 4202-4206.

14 Hajeeth T, Gomathi T & Sudha P N, Adsorption of Cr(VI) from aqueous solution using cellulose extracted from sisal fiber, *Indian J App Res*, 3 (2013) 1-5.

15 Teoh Wah T, Takuma T & Kazunori S, Sorption of Pb(II), Cd(II), and Ni(II) Toxic Metal Ions by Alginate-Bentonite, *J Environ Prot*, 4 (2013) 51-55.

16 Qasem Naef A A, Ramy H M & Dahiru U L, Removal of heavy metal ions from wastewater: A comprehensive and critical review, *Npj Clean Water*, 4 (1) (2021) 1-15.

17 Aydin Y A & Aksoy N D, Adsorption of chromium on chitosan: Optimization, Kinetics and thermodynamics, *Chem Eng J*, 151 (2009) 188-194.

18 Nithya R, Gomathi T, Sudha P N, Venkatesan J, Sukumaran A, *et al.*, Removal of Cr(VI) from aqueous solution using chitosan-g-poly(butylacrylate)/silica gel nanocomposite, *Int J Biol Macromolec*, 87 (2016) 545–554.

19 Kyzas G K, Kostoglou M & Lazaridis N K, Copper and Chromium (VI) removal by chitosan derivatives- Equilibrium and kinetic studies, *Chem Eng J*, 152 (2009) 440-448.

20 Sivakami M S, Gomathi T, Venkatesan J, Hee-Seok J, Se-kwon K, *et al.*, Preparation and characterization of nano chitosan for treatment wastewaters, *Int J Biol Macromolec*, 57 (2013) 204-212.

21 Rajiv G M, Kousalya G N & Meenakshi S, Removal of copper(II) using chitin/chitosan nano-hydroxyapatite composite, *Int J Biol Macromolec*, 48 (2011) 119-124.

22 Jayakumar R, Prabaharan M, Reis R L & Mano J F, Graft copolymerized chitosan—present status and applications, *Carbohydr Polym*, 62 (2005) 142-158.

23 Shukla S K, Mishra A K, Arotiba O A & Mamba B B, Chitosan –based nanomaterials: A state-of –the-art review, *Int J Biol Macromolec*, 59 (2013) 46-58.

24 Zuoying C, Huacai G & Shengli L, Studies on synthesis and adsorption properties of chitosan cross-linked by glutaraldehyde and Cu (II) as template under microwave irradiation, *Eur Polym J*, 37 (2001) 2141-2143.

25 Rojas G, Silva J, Flores J A, Rodriguez A, Ly M, *et al.*, Adsorption of chromium onto cross-linked chitosan, *Sep Purif Tech*, 44 (2005) 31-36.

26 Nalini S, Awantika D, Leela I & Rashmi S, Removal of hexavalent chromium using a novel cross linked xanthated chitosan, *Bioresour Technol*, 97 (2006) 2377-2382.

27 Wei W, Yang L, Zhong W, Cui J & Wei Z, Poorly crystalline hydroxyapatite: A novel adsorbent for enhanced fulvic acid removal from aqueous solution, *Appl Surf Sci*, 332 (2015) 328–339.

28 Yu X, Tong S, Ge M & Zuo J, Removal of fluoride from drinking water by celluloe@hydroxyapatite nanocomposites, *Carbohydr Polym*, 92 (2013) 269-275.

29 Krishna K A S, Shruti S K & Rajesh N, A novel amine impregnated graphene oxide adsorbent for the removal of hexavalent chromium, *Chem Eng J*, 230 (2013) 328-337.

30 Harijan D K L & Chandra V, Polyaniline functionalized graphene sheets for treatment of toxic hexavalent chromium, *J Environmental Chem Eng*, 4 (2016) 3006-3012.

31 *Pan Y, Wu T, Bao H & Li L,* Green fabrication of chitosan films reinforced with parallel aligned graphene oxide, *Carbohydr Polym*, 83 (2011) 1908-1915.

32 Liu L, Li C, Bao C, Jia Q, Xiao P, et al., Preparation and characterization of chitosan/grapheme oxide composites for the adsorption of Au(III) and Pb(II), Talanta, 93 (2012) 350-357.

33 Li B, Shan C L, Zhou Q, Fang Y, Wang Y L, *et al.*, Synthesis, Characterization, and Antibacterial Activity of Cross-Linked Chitosan-Glutaraldehyde, *Mar Drugs*, *11* (*2013)* 1534-1552.

34 Monteiro O A C & Airoldil C, Chitosan based nanomaterial-A state- of -the- art- review, *Int J Biol Macromolec*, 59 (2013) 46-58.

35 Azzaoui K, Lamhamdi A, Mejdoubi E M, Berrabah M, Hammouti B, *et al*., Synthesis and characterization of composite based on cellulose acetate and hydroxyapatite application to the absorption of harmful substances, *Carbohydr Polym*, 111 (2014) 41-46.

36 Hu F, Wang X, Wang J, Liu F, Zhang M, *et al.*, Microwave-assisted covalent modification of graphene nanosheets with chitosan and its electrorheological characteristics, *Appl Surf Sci*, 257 (2011) 2637-2642.

37 Gower L B, Biomimetic model systems for investigating the amorphous precursor pathway and its role in biomineralization, *Chemical reviews*, 108 (11) (2008) 4551-4627.

38 Neelgund G M, Oki A & Luo Z, In situ deposition of hydroxyapatite on grapheme nanosheets, *Mater Res Bull*, 48 (2013) 175-179.

39 Venkatesan J, Zhong-Ji Q, BoMi R, Nanjundan A K & Se-Kwon Kim, Preparation and characterization of carbon nanotube-grafted-chitosan–natural hydroxyapatite composite for bone tissue engineering, *Carbohydr Polym*, 83 (2011) 569-577.

40 Justin R & Chen B, Body temperature reduction of graphene oxide through chitosan functionalisation and its application in drug delivery, *Mater Sci Eng C*, 34 (2014) 50-53.

41 Jankovic A, Erakovic S, Mitric M, Matc I Z, Juranic Z D, *et al*., Bioactive hydroxyapatite/graphene composite coating and its corrosion stability in simulated body fluid, *J Alloys Compd*, 624 (2015) 148-157.

42 Sun Y, Yue Q, Mao Y, Gao B, Gao Y, *et al.*, Enhanced adsorption of chromium onto activated carbon by microwave assisted H_3PO_4 mixed with Fe/Al/Mn activation, *J Hazard Mater*, 265 (2014) 191-200.

43 Ayawei N, Augustus N E & Donbebe W, Modelling and interpretation of adsorption isotherms, *J Chem*, 2017 (2017) pp. 11.

44 Wassel M, Swlem S A, Hamoda S & Desouky A, Studies on the preparation modified chitosan and its applications, *Al-azhar Bull Sci*, 24 (1) (2013) 33-48.

45 Liu X & Zhang L, Removal of phosphate anions using the modified chitosan beads: Adsorption kinetic, isotherm and mechanism studies, *Powder Technol*, 277 (2015) 112-119.